



**HAL**  
open science

# **Pervasive LPWAN connectivity through LEO Satellites: trading off reliability, throughput, latency, and energy efficiency**

Zheng Zhou, Mohammad Afhamisis, Maria Rita Palattella, Nicola Accettura,  
Pascal Berthou

## ► To cite this version:

Zheng Zhou, Mohammad Afhamisis, Maria Rita Palattella, Nicola Accettura, Pascal Berthou. Pervasive LPWAN connectivity through LEO Satellites: trading off reliability, throughput, latency, and energy efficiency. Ismail Butun; Ian F. Akyildiz. Low-Power Wide-Area Networks: Opportunities, Challenges, Risks and Threats, Springer, In press, 978-3-031-32934-0. hal-03844534v2

**HAL Id: hal-03844534**

**<https://laas.hal.science/hal-03844534v2>**

Submitted on 17 Apr 2023

**HAL** is a multi-disciplinary open access archive for the deposit and dissemination of scientific research documents, whether they are published or not. The documents may come from teaching and research institutions in France or abroad, or from public or private research centers.

L'archive ouverte pluridisciplinaire **HAL**, est destinée au dépôt et à la diffusion de documents scientifiques de niveau recherche, publiés ou non, émanant des établissements d'enseignement et de recherche français ou étrangers, des laboratoires publics ou privés.

311 **Chapter 1**  
312 **Pervasive LPWAN connectivity through LEO**  
313 **Satellites: trading off reliability, throughput,**  
314 **latency, and energy efficiency**

315 Zheng Zhou, Mohammad Afhamisis, Maria Rita Palattella, Nicola Accettura and  
316 Pascal Berthou

317 **Abstract** With the increasing success of the Internet of Things (IoT) industry  
318 and the consequent conception of new IoT applications, a significant variety of  
319 network design challenges has been unfolded. As a consequence, different Low Power  
320 Wide Area Networks (LPWAN) technologies have been developed and marketed to  
321 address each specific application need. Among them, the Narrowband IoT (NB-IoT)  
322 was developed to target reliable communications over the licensed spectrum, while  
323 the Long Range (LoRa) was conceived as a loss-tolerant means over unlicensed  
324 frequencies. Recently, satellite LPWAN appeared as a new connectivity option and  
325 an affordable solution, particularly suitable for remote and not easily accessible areas.  
326 This book chapter timely addresses the opportunities and challenges of such satellite  
327 LPWAN architecture by providing a general framework for the evaluation of its  
328 performances. The chapter also describes a methodological approach for designing  
329 the network, selecting the configuration parameters and the traffic patterns, fitting  
330 the best trade-off among reliability, latency, throughput, and energy efficiency.

331 **1.1 Introduction**

332 Low Power Wide Area Network (LPWAN) is becoming a revolutionary technology  
333 for the Internet of Things (IoT) due to its low power consumption, long distance  
334 coverage, and low cost of the devices [19]. Many LPWAN technologies have been

---

Zheng Zhou, Nicola Accettura and Pascal Berthou  
Laboratory for Analysis and Architecture of Systems (LAAS-CNRS), Université de Toulouse,  
CNRS, UPS, Toulouse, France  
emails: {name.surname}@laas.fr

Mohammad Afhamisis and Maria Rita Palattella  
Environmental Research and Innovation Department (ERIN), Luxembourg Institute of Science and  
Technology (LIST), Esch-sur-Alzette, Luxembourg  
emails: {name.surname}@list.lu

335 developed over the last few years. 3GPP standardized Cat-M and Narrow Band  
336 IoT (NB-IoT) [2], two complementary technologies targeting reliable applications  
337 over the licensed spectrum. At the same time, the unlicensed spectrum was recently  
338 populated by other loss tolerant LPWAN technologies, quickly dominating the IoT  
339 landscape and market for their easy deployment. Among them, Sigfox[1] and the  
340 Long Range (LoRa) technology [3].

341 With the cost reduction of CubeSat Low Earth Orbit (LEO) satellites, and the  
342 low latency achievable with large LEO constellations, satellite LPWAN recently  
343 became a new solution to connect a large set of IoT devices deployed in remote  
344 and even inaccessible areas [16]. Many IoT companies and satellite operators have  
345 invested a lot in making such a solution feasible. While few real deployments already  
346 exist, many research challenges still need to be addressed to make such network  
347 architecture a reality and bring IoT connectivity everywhere [43]. Clearly, satellite  
348 communications are still unable to support the low-latency requirements demanded  
349 by some IoT applications, like mission-critical applications, tactile Internet, factory  
350 automation, and Ultra-Reliable and Low-Latency (URLLC) systems [20]. On the  
351 contrary, they can easily meet the requirements of delay-tolerant applications, such  
352 as smart agriculture, smart grid, cross-border tracking systems, and maritime Internet  
353 of Things [52] and surveillance [34].

Interestingly, both LoRa and NB-IoT are highly configurable protocols that provide the possibility to choose among multiple link layer communication schemes to tackle different reliability requirements. Higher reliability is usually achieved at the price of larger latency. Notably, this trade-off between reliability and latency is highly susceptible to the amount of offered traffic, making the network throughput an additional element to be taken into account when designing the network. As a matter of fact, reliability, latency, and throughput are the three main Key Performance Indicators (KPIs) for any communication network [48]. Remarkably, the subset of IoT networks is featured by an additional KPI, i.e., energy efficiency. Indeed, a typical IoT network includes numerous cheap smart devices equipped with batteries, whose most energy-expensive activity is related to the radio module. Hence, IoT communication protocols should be designed to prolong the battery lifetime without requiring frequent substitutions or recharges. All in all, trading-off among reliability, latency, throughput and energy efficiency results as the sole approach able to tackle the need of any application. In this book chapter, a methodological approach to evaluate the performance of a satellite LPWAN network is presented, considering the challenges introduced by satellites.

354 The rest of the chapter is organized as follows. Sec. 1.2 introduces and compares  
355 NB-IoT and LoRa technologies by highlighting those technological facets making  
356 them easily exploitable for ground-to-satellite low power communications. Then,  
357 Sec. 1.3 investigates how the communication KPIs are strictly dependent on a set  
358 of parameters, with some of them being unmodifiable physical properties and the  
359 others being configurable protocol settings. Sec. 1.4 describes the opportunities and

360 challenges inherent to the integration of LPWAN with LEO satellites. Sec. 1.5 shows  
 361 how the LPWAN KPIs are impacted by the satellite features. Finally, Sec. 1.6 draws  
 362 conclusions and envisages future research directions.

## 363 1.2 LPWAN Technologies: LoRa vs NB-IoT

364 In the IoT landscape, the Low Power Wide Area Network (LPWAN) technology  
 365 emerged as the best choice for enabling very low-cost long-range connections. Many  
 366 LPWAN technologies have been developed over the last years, e.g., LoRa, Sigfox,  
 367 NB-IoT, and CAT-M. This chapter focuses on LoRa and NB-IoT, whose integration  
 368 with LEO satellites has already been investigated in the research community and  
 369 partly implemented in the context of ongoing 3GPP work items [16]. Since the  
 370 approach described throughout this chapter aims at picturing the integration of any  
 371 LPWAN technology on ground-to-satellite IoT links, the key features of LoRa and  
 372 NB-IoT are described in parallel according to a comprehensive mindset, in order  
 373 to provide useful insights for the proper choice of the most fitting communication  
 374 pattern. To help the reading, a very high-level comparison is provided in Table 1.1.

Table 1.1: Comparative Matrix: NB-IoT vs LoRaWAN

<i>Feature \ Technology</i>	<b>LoRaWAN</b>	<b>NB-IoT</b>
<i>Specifications</i>	Non-3GPP	3GPP
<i>Uplink Modulation</i>	CSS	SC-FDMA
<i>Downlink Modulation</i>	CSS	OFDM
<i>Frequency Band</i>	ISM unlicensed band	Cellular licensed band
<i>Bandwidth</i>	125/250/500 kHz	180 kHz
<i>Maximum Data Rate</i>	50 kbps	200 kbps
<i>Coverage Range</i>	5-20km [42]	1-10km
<i>Security</i>	AES 128 bit	3GPP(128-256 bit)

375 In details, **LoRa** was introduced by Semtech Corporation <sup>1</sup> and adopts a *Chirp*  
 376 *Spread Spectrum* (CSS) modulation scheme to enable long range communication  
 377 even in noisy environments [35]. Herein, a narrowband input signal is spread over  
 378 a wider bandwidth and immediately transmitted; then, it can be correctly decoded  
 379 very far away, even if severely attenuated. The LoRa modulation further enables  
 380 the use of several Spreading Factors (SFs) to increase the ability of the receiver to  
 381 decode simultaneous signal transmissions on the same frequency channel. Each SF  
 382 is associated with a specific data-rate, transmission range, and energy consumption.  
 383 Such communications happen on the *unlicensed* Industrial, Scientific, and Medical  
 384 (ISM) *band*, thus competing for the use of the radio resources with other interfer-  
 385 ing technologies operating in the same frequency bands. The enormous interest of

<sup>1</sup> Semtech: <https://www.semtech.com/lora>

386 companies on such a cutting-edge technology pushed for the creation of the LoRa  
387 Alliance with the aim of promoting LoRa and designing a Medium Access Control  
388 (MAC) layer able to manage the communication resource exploitation in LoRa Wide  
389 Area Networks (LoRaWAN). The LoRaWAN protocol was initially defined as an  
390 open specification for LPWAN IoT, and, in December 2021, it has been finally rec-  
391 ognized as a standard by the International Telecommunication Union (ITU <sup>2</sup>). The  
392 transposition as an ITU-T Recommendation (ITU-T Y.4480) validates the market  
393 trend in adopting LoRaWAN as an internationally recognized standard and defines  
394 the path ahead toward even wider adoption. More interestingly, several companies  
395 have been working with Semtech to ensure a pervasive availability of IoT services  
396 through LEO satellites equipped with LoRa transceivers. Among such companies,  
397 it is worth mentioning Lacuna Space <sup>3</sup>, Thuraya <sup>4</sup>, ACTILITY <sup>5</sup>, and WYLD <sup>6</sup>.

398 Instead, **NB-IoT** employs a *narrow band modulation* and works into the *licensed*  
399 *spectrum*. It was conceived by 3GPP and proposed for the first time in Release  
400 13 [2] to make current cellular networks ready to support IoT applications with  
401 low cost, low power consumption, and low data rates. The development of the  
402 NB-IoT standard was initially based on the existing Long-Term Evolution (LTE)  
403 functionalities. Such an approach (i.e., leveraging on existing technology) allowed  
404 minimizing the development effort and shortening the time to market. The NB-IoT  
405 specification is still evolving, and the most recent releases, i.e., Rel-17 and Rel-  
406 18, focus on IoT over Non-Terrestrial Networks (NTN) to provide broader global  
407 coverage. Their objective is to address the challenges inherent to the integration of  
408 NB-IoT over ground-to-satellite links, i.e., initial synchronization, high propagation  
409 delays, Doppler variation rate, high paging load with a considerable number of users,  
410 etc. Several companies, like Sateliot<sup>7</sup>, Ligado <sup>8</sup>, and GateHouse<sup>9</sup>, have invested in  
411 designing and developing global NB-IoT satellite networks and can already offer  
412 such service.

413 From the **Network Architecture** point of view, LoRaWAN and NB-IoT present a  
414 similar hierarchical structure with two tiers, as depicted in Fig. 1.1. With LoRaWAN,  
415 low power End Devices (EDs) communicate through LoRa links with all the Lo-  
416 RaWAN Gateways (GWs) in their transmission range. The GWs are totally controlled  
417 by the LoRaWAN Network Server (LNS), and their function is to encapsulate uplink  
418 LoRa frames received by EDs within TCP/IP packets and forward them to the LNS.  
419 The GWs also forward the downlink traffic from LNS to EDs. In fact, the LoRaWAN  
420 MAC protocol is established between any ED and the LNS. In turn, the LNS can be  
421 interconnected with several application servers.

<sup>2</sup> LoRaWAN® Formally Recognized as ITU International Standard for Low Power Wide Area Networking: <https://lora-alliance.org/lora-alliance-press-release/>

<sup>3</sup> Lacuna Space: <https://lacuna.space/>

<sup>4</sup> Thuraya: <https://thuraya.com/>

<sup>5</sup> Actility: <https://www.actility.com/>

<sup>6</sup> Wyld networks: <https://wyldnetworks.com/>

<sup>7</sup> Sateliot: <https://sateliot.space/en/>

<sup>8</sup> Ligado: <https://ligado.com/>

<sup>9</sup> Gatehouse: <https://gatehouse.com/>

422 Similarly, the NB-IoT network architecture can be divided into two main parts:  
 423 the core network, namely the Evolved Packet Core (EPC), and the access network,  
 424 namely the Evolved Universal Terrestrial Radio Access Network (E-UTRAN). EPC  
 425 is responsible for transmitting the collected IoT data to the cloud platform for further  
 426 processing and managing mobile devices [2].

427 The access network includes the User Equipment (UE) and the evolved Node B  
 428 (eNB). Clearly, an NB-IoT UE plays the same network role as a LoRaWAN ED.  
 429 Indeed, UEs and EDs are equipped with one or more sensors, a microcontroller, and  
 430 a radio transceiver, and they are in charge of collecting and transmitting IoT data  
 431 to the Internet through respectively the EPC and the LNS. Instead, the eNB (as the  
 432 LGW) is the base station connecting the UE to the core network.

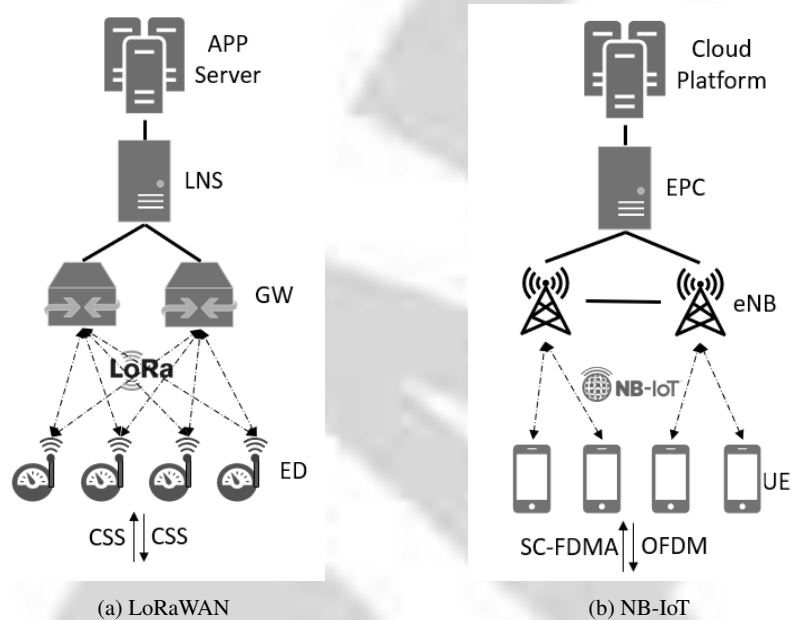


Fig. 1.1: Comparison between NB-IoT and LoRaWAN architectures

433 From the perspective of **physical layer**, LoRa achieves long range transmissions  
 434 up to  $\sim 20\text{km}$  thanks to the CSS modulation [42]. When an ED has some data to  
 435 transmit, the signal is spread over the air using a specific bandwidth (BW) and SF.  
 436 According to the LoRaWAN specification, the SF can assume integer values from 7  
 437 to 12. The SF impacts other two parameters of the LoRa PHY layer protocol, i.e.,  
 438 the Data Rate (DR) and the Time on the Air (ToA). The DR is the number of bytes  
 439 transmitted per second on the air. The ToA is the amount of time for a message  
 440 to be delivered to the GW, and its length is directly proportional to the size of the  
 441 transmitted frame and inversely proportional to the DR.

442 The LoRa DR can be calculated as

$$DR = SF \times \frac{Bandwidth}{2^{SF}} \times CR. \quad (1.1)$$

443 The CR is the code rate, which is a fractional number that represents the proportion  
 444 of useful (non-redundant) data in the encoded data stream to the total encoded  
 445 data. In fact, a higher SF allows a longer coverage range and a higher resilience  
 446 against noise. However, according to the Equation 1.1, this comes at the cost of  
 447 a smaller DR, that in turn implies a longer ToA and larger energy consumption.  
 448 To overcome such limitations, Semtech recently designed a new LoRa PHY layer,  
 449 namely Long-Range Frequency Hopping Spread Spectrum (LR-FHSS), also known  
 450 as LoRa-Extended [15]. The LR-FHSS operates in the same channels as the regular  
 451 LoRa PHY. But the LoRa bandwidth is divided into several smaller ones, named  
 452 hops. In LR-FHSS, ED and GWs get synchronized using a pseudo random sequence,  
 453 which specifies the specific hops to use for the data transmission. This sequence  
 454 is exchanged using a header, with two or three replicas sent in randomly selected hops.  
 455 Once the synchronization is established, then the ED starts transmitting the payload,  
 456 which is divided into several small portions named *fragments*. Each fragment is sent  
 457 over a different hop, following the pseudo random sequence previously exchanged.  
 458 This results in a longer ToA, for transmitting the same payload, compared to the  
 459 LoRa PHY (see Fig. 1.2). It must be noticed that LR-FHSS applies only to the uplink  
 460 transmission. Downlink traffic still follows the regular LoRa PHY.

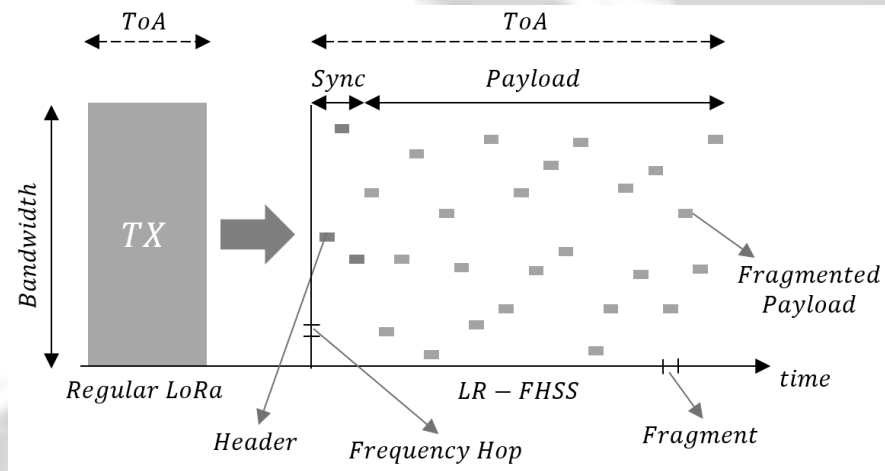


Fig. 1.2: LoRa PHY vs LR-FHSS

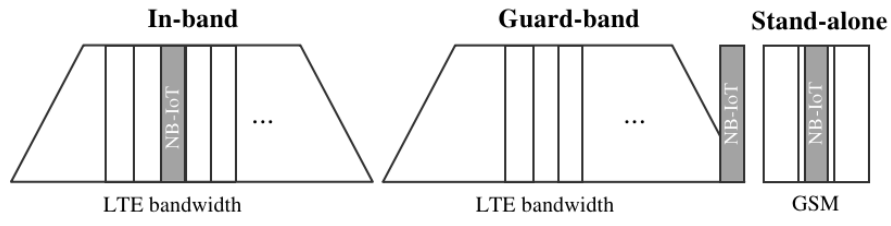


Fig. 1.3: NB-IoT deployment modes

### > Important

461

462 However, since LoRa uses the unlicensed ISM band, the duty cycle must be con-  
 463 figured to limit the maximum amount of data each device can upload daily, while  
 464 respecting the access policies. In Europe, the European Telecommunications Stan-  
 465 dards Institute (ETSI) enforces per sub-band duty cycle policies ranging from 0.1%  
 466 to 10% [26]. In the Federal Communications Commission (FCC) regions, a max-  
 467 imum ToA of  $400ms$  is imposed, for the uplink transmissions, while there is no  
 468 restriction on the duty cycle. Finally, concerning the bandwidth, 125 kHz can be  
 469 adopted in both regions, while 250 kHz and 500 kHz are allowed in the ETSI and  
 470 FCC regions, respectively.

471

472 Like LTE, and differently from LoRa, NB-IoT adopts two different modulation  
 473 schemes for downlink and uplink messages, respectively Orthogonal Frequency-  
 474 Division Multiple Access (OFDMA), and Single Carrier-Frequency Division Multi-  
 475 ple Access (SC-FDMA). NB-IoT occupies the 180 kHz frequency band, correspond-  
 476 ing to a block of resources in the LTE bandwidth. NB-IoT supports three deployment  
 477 modes, illustrated in Fig. 1.3. The In-band mode occupies one of the Physical Re-  
 478 sources Blocks (PRBs) of LTE. The Guard-band mode occupies only the protection  
 479 band of LTE. In the stand-alone mode, NB-IoT can be deployed in any frequency  
 480 spectrum, such as Global System for Mobile (GSM) frequency bands.

481 Fig. 1.4 illustrates the structure of NB-IoT radio frame. Each radio frame has a  
 482 duration of 10 ms and is divided into 10 subframes. Each subframe is made up of  
 483 2 slots. One subframe consists of  $12 \times 14$  Resource Elements (REs) with a 15 kHz  
 484 subcarrier for downlink (3.75 kHz or 15 kHz for uplink). 3GPP has defined several  
 485 channels and signals with distinct functions for uplink and downlink, as described  
 486 hereafter.

487 For the downlink, as shown in Fig. 1.5, two synchronization signals, Narrowband  
 488 Primary Synchronization Signal (NPSS) and Narrowband Secondary Synchroniza-  
 489 tion Signal (NSSS), are transmitted in the subframes 5 and 9 to synchronize UE and  
 490 eNB in time and frequency. The first subframe is Narrowband Physical Broadcast  
 491 Channel (NPBCH), which is used to exchange critical system information such as  
 492 deployment mode. The remaining subframes are occupied by the other two chan-



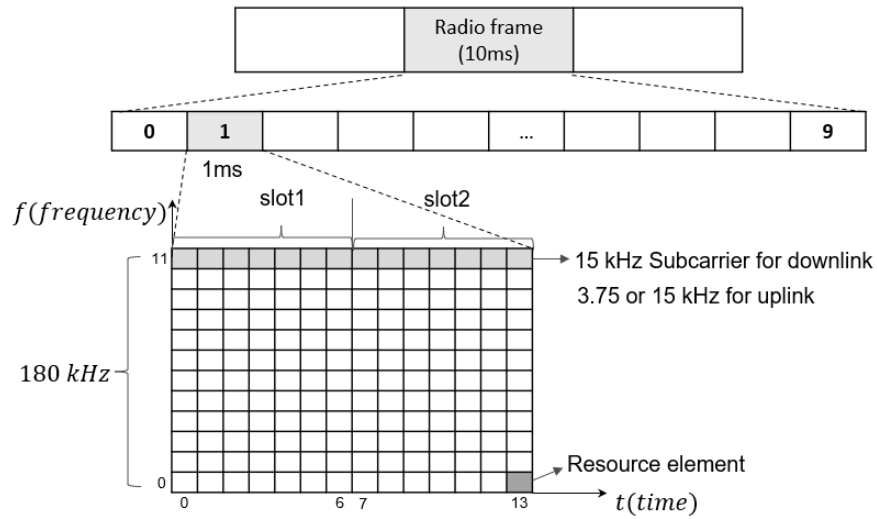


Fig. 1.4: Radio Frame of NB-IoT

493 nels: Narrowband Physical Downlink Control Channel (NPDCCH) and Narrowband  
 494 Physical Downlink Shared Channel (NPDSCH). The control channel contains infor-  
 495 mation on uplink and downlink resource scheduling, allowing the UE to know when  
 496 to receive or send messages. In the shared channel, downlink data and other system  
 497 messages are exchanged. Note that control and shared channels may occupy several  
 498 subframes, depending on the size of the message, the number of repetitions, etc.

499 Two different channels are defined for uplink transmission, as also pictured in  
 500 Fig. 1.5. The first connection attempt (Random access preamble) of the UE to the  
 501 eNB is transmitted in Narrowband Physical Random Access Channel (NPRACH),  
 502 where the collision happens. The uplink data is transmitted in Narrowband Physical  
 503 Uplink Shared Channel (NPUSCH). Those resources are allocated by the upper  
 504 layer avoiding a-priori any collision. Therefore, this channel is also known as a non-  
 505 contention channel. Finally, NB-IoT supports two transmission modes: Multiton and  
 506 Singleton. Singleton uplink messages occupy only one subcarrier, while Multiton  
 507 uplink messages occupy multiple (3, 6, 12) subcarriers. So multiple UEs can occupy  
 508 the same channel, allowing more users to be connected simultaneously.

509 Unlike NB-IoT, in a LoRaWAN network EDs do not negotiate the resource allo-  
 510 cation with the GW, but they still need to join the network, before being able to  
 511 transmit the data. To this aim, they should exchange some keys with the LNS, and  
 512 ensure the secure data exchange over the end-to-end system. As shown in Fig. 1.6,  
 513 two different join procedures are supported by the standard: Activation Before Per-  
 514 sonalization (ABP) and Over The Air Activation (OTAA). In the ABP, the keys are  
 515 pre-stored in the ED. When there is a message to send, the keys are sent along with  
 516 the data and authenticated by the LNS. Instead, in the OTAA mode, the EDs need

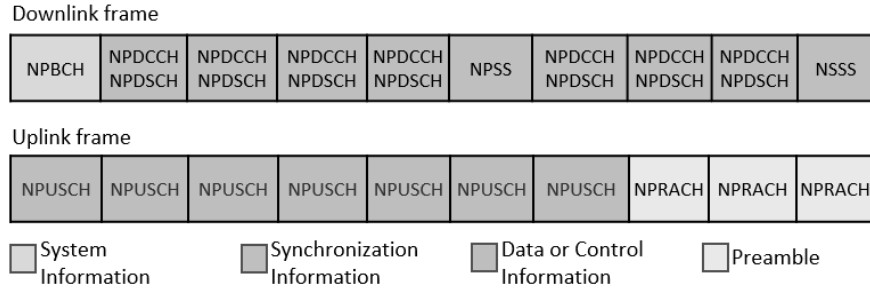


Fig. 1.5: Downlink and uplink frames of NB-IoT

517 to send a *join request* and receive *join accept* from the LNS, before being accepted  
 518 in the network.

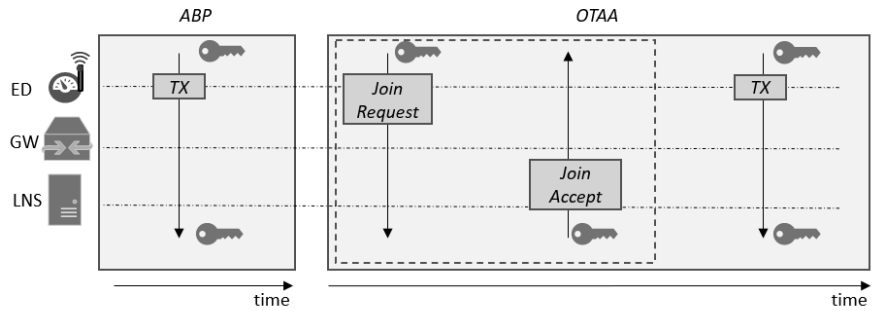


Fig. 1.6: LoRaWAN Join procedures: OTAA vs ABP.

519 The LoRaWAN protocol adopts an ALOHA-based random-access scheme [46] as  
 520 **Medium Access Control Protocol**. EDs transmit without listening and sensing the  
 521 channel before. The LoRa EDs can operate in three different communication classes,  
 522 illustrated in Fig. 1.7. Class A is the simplest mode and the default class, supported  
 523 by all the EDs. After each uplink transmission, two receive windows,  $Rx1$  and  $Rx2$ ,  
 524 are opened, allowing the ED to receive downlink traffic from the LNS through the  
 525 GW. The ED waits for  $1s$  before opening the  $Rx1$ . If the ED cannot receive any  
 526 downlink in the  $Rx1$ , then it opens the  $Rx2$ , after an additional delay of  $1s$ . The ED  
 527 switches into sleep mode after  $Rx2$ , till the next uplink has started. The class C is  
 528 like Class A, with the difference that the receiving windows are never closed, and  
 529 they stay open till the next uplink. Thus, the class C is less energy-efficient than Class  
 530 A. In Class B, the EDs use beacon messages sent from the GW to synchronize with  
 531 the LNS. It allows the EDs to open additional receive windows, named ping slots,

532 without the need of prior uplink transmission. Since ED must be in RX mode during  
 533 the ping slots, Class B implies additional energy consumption compared to Class A.  
 534 It must be noticed that Class B devices still operate like Class A devices for uplink  
 535 transmissions.

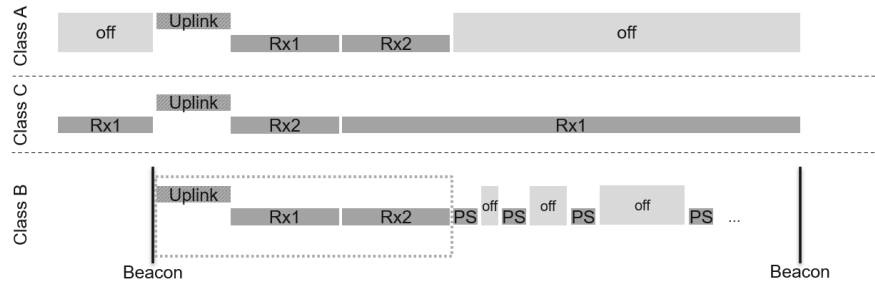


Fig. 1.7: The LoRaWAN communication mode: Classes A, B and C.

536 The UE of the NB-IoT must synchronize with the eNB by receiving the synchron-  
 537 ization signals before connecting with the eNB. For LoRa, only Class B enables  
 538 the synchronization between the ED and the GW using beacons.

539 When a UE is covered by more than one eNB simultaneously, it measures the  
 540 received power and then selects the one with the best available coverage (best signal  
 541 quality). In LoRa, the ED transmits to any gateways in its coverage range. It is up  
 542 to the LNS to select the best gateway for sending back downlink traffic. Moreover,  
 543 while in LoRaWAN, the ED receives the configuration parameters from the LNS, in  
 544 an NB-IoT network, the UE itself determines the Coverage Enhancement (CE) level  
 545 according to its distance from the eNB and thus, chooses the number of repetitions  
 546 of a message (2-1024 times). The higher the CE level (0-2), the higher the power  
 547 consumption of the data transmission [32].

548 When the UE has a message to send or monitors paging, it will connect to the eNB  
 549 as shown in Fig. 1.8. The random-access process will begin once the UE completes  
 550 the synchronization with the eNB. A random-access preamble is sent to the eNB  
 551 using the random-access channel (Msg1). The UE starts a timer and waits for a  
 552 random-access response (Msg2). If no response is received, the UE will send a new  
 553 preamble. After a successful reception of Msg2, Msg3 is sent from the UE to the eNB,  
 554 which holds control information of radio resources, data volume, reconfiguration  
 555 request, etc. Msg4 is the connection setup and the contention resolution, where the  
 556 eNB accepts to establish the connection with a UE. After receiving Msg4, the UE  
 557 will enter the connected state from the idle state. Then the eNB and UE exchange  
 558 messages for authentication and AS security configuration (Msg6-9). After that,  
 559 UE sends its uplink data and receives downlink data. Finally, the eNB releases the  
 560 connection if it detects inactivity from the UE (Msg10).

561 NB-IoT defines two optimization methods for data transmission to reduce message  
 562 exchange: the User Plane (UP) and the Control Plane (CP) optimization. The CP

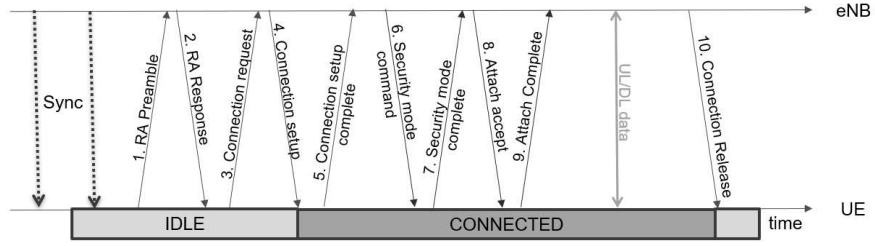


Fig. 1.8: NB-IoT Workflow

563 carries the signaling responsible for accessing the UE, allocating resources (e.g.,  
 564 messages exchanged after random access), etc.; the UP carries the user data.

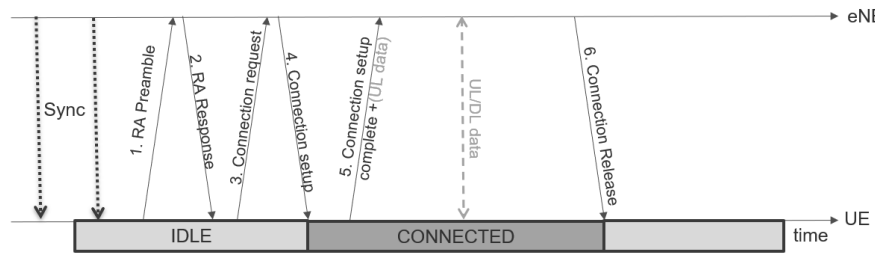


Fig. 1.9: NB-IoT CP optimization

565 It must be noticed that for sending and receiving a few bytes of data, the signaling  
 566 overhead consumed by the UE from the idle state to the connected state is much  
 567 more significant than the data load. To make data transmission more efficient, two  
 568 optimization schemes have been proposed: Control Plane (CP) and User Plane (UP)  
 569 optimization. With the CP optimization shown in Fig. 1.9, small packets can be added  
 570 to the control message (Msg5) and bypass the security configurations to improve the  
 571 speed for transferring small data. This mode is insecure compared to other modes.

572 The UP optimization allows idle users to transfer data quickly through the *suspend*  
 573 *and resume* process. After establishing the first connection (see Fig. 1.10), the user's  
 574 information can be stored in the eNB. No Connection Release message is transmitted.  
 575 When there is new data to transfer, the UE can soon recover the connection without  
 576 re-establishing the security information.

577 In Release 15, 3GPP defined the *Early Data Transmission* (EDT) mode to reduce  
 578 UE energy consumption and message latency by reducing the number of transmis-  
 579 sions [33]. Specified for both UP and CP optimization, the EDT can be used when  
 580 the UE is in idle mode and has less than the maximum broadcast uplink data to send.

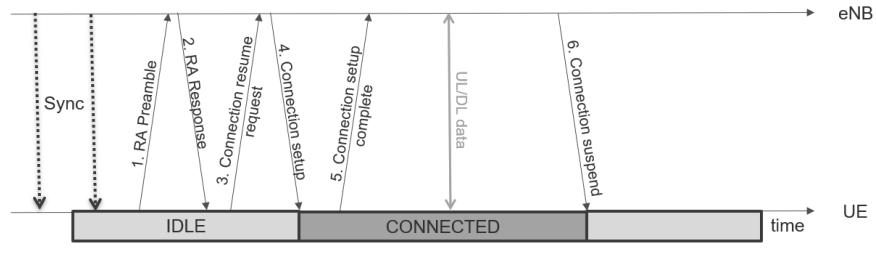


Fig. 1.10: NB-IoT UP optimization

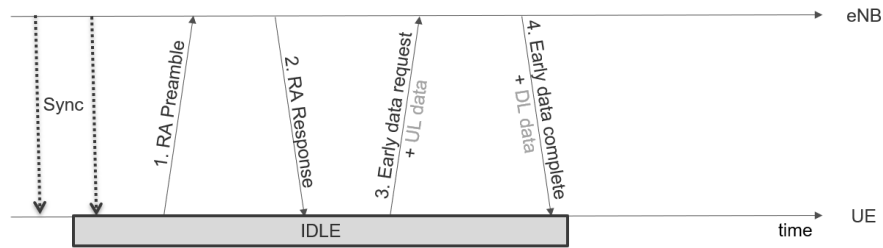


Fig. 1.11: NB-IoT Early Data Transmission

582 In this mode, only four messages between the eNB and the UE are required to  
 583 complete the data transmission because the data is sent during the random-access  
 584 procedure. As shown in Fig. 1.11, the data is included in Msg3. The method of  
 585 encapsulating and transmitting uplink data is like the optimization of the CP. If the  
 586 UE receives the Msg4 indicating that the procedure is terminated, it can go to the  
 587 sleep state or stay in the idle state.

588 Thanks to more complex synchronization and resource allocation techniques,  
 589 NB-IoT can offer higher reliability compared to LoRa. This is paid with (i) longer  
 590 transmission delays, which can be reduced using CP, UP optimization, and EDT;  
 591 and (ii) higher energy consumption for the IoT device. LoRa, while being more  
 592 energy-efficient, it suffers from high collision probability due to the random-access  
 593 mechanism. Both reliability and throughput can be improved using resource allocation  
 594 schemes, like TDMA approaches.

595 In the following, an in-depth analysis of the performance achievable with the two  
 596 technologies is conducted in order to identify key protocol metrics impacting the  
 597 performance.

### 598 1.3 Methodological Approach for Performance Evaluation

599 Evaluating the performances of NB-IoT and LoRaWAN is the very first step to  
 600 effectively comparing their modes of operation. Then, the best communication pro-  
 601 tocol can be selected to fit the target application's requirements expressed as a set  
 602 of Key Performance Indicators (KPI). Remarkably, the typical KPIs for network  
 603 performance evaluation are **Reliability**, **Latency**, and **Throughput** [48].

604 As already discussed in Section 1.1, IoT networks require the evaluation of another  
 605 important KPI, i.e., **Energy Efficiency**. In this chapter, only these four most critical  
 606 KPIs for LPWAN will be discussed and analyzed. The importance of evaluating  
 607 all these aspects to choose the most fitting network technology can be intuitively  
 608 understood as follows. NB-IoT is designed to be a reliable, delay-tolerant protocol  
 609 on the licensed spectrum, while LoRa is a loss-tolerant protocol. Hence, they provide  
 610 different link-layer solutions for different needs, making it possible to choose between  
 611 reliable and delay-constrained protocols.

612 With the goal of deeply understanding which parameters affect the identified  
 613 KPIs, this section focuses on the analysis of the LPWAN terrestrial network, while  
 614 an extension to ground-to-satellite communications will be discussed in the following  
 615 sections.

Table 1.2: Comparison of the models and their KPIs

<i>KPI \ Models</i>	<b>NB-IoT</b>	<b>LoRaWAN</b>
<i>Reliability</i>	[37] [11] [24]	[9] [39] [38] [12] [23] [50]
<i>Latency</i>	[40] [37] [7] [8]	[9] [50]
<i>Throughput</i>	[49] [40] [24]	[9] [12] [39]
<i>Energy Efficiency</i>	[40] [7] [8] [10]	[45] [41]

616 The most recent works on LPWAN modelling that drove the identification of the  
 617 KPIs are listed in Table 1.2. Instead, Table 1.3 summarises the mathematical notation  
 618 used in this section, and throughout the entire chapter.

619 First of all, a communication protocol is reliable if the transmitter can be notified  
 620 through an acknowledgement (ACK) about the correct delivery of data frames from  
 621 the receiver. The lack of any ACK mechanism makes the communication protocol  
 622 unreliable. This is the case of unconfirmed Class A LoRaWAN frame transmissions.

Instead, the portion of acknowledged transmissions provides a measure of the **Reliability** of the communication protocol [31]. Such a KPI can be evaluated for LoRaWAN confirmed-based communications and for NB-IoT. When the analyzed protocol enables re-transmission of unacknowledged frames up to a maximum of  $M$  times, then the reliability  $R$  of the protocol is

$$R = 1 - PLR^M, \quad (1.2)$$

where  $PLR$  is the measured Packet Loss Ratio.

623 Clearly, being the PLR a positive real number lower than 1, a higher value for  $M$   
 624 translates into increased communication reliability [37]. At the same time, a higher  
 625 PLR negatively impacts such a KPI. As a consequence, the communication reliability  
 626 can be kept over a given threshold value by properly tuning either the maximum  
 627 number of retransmissions  $M$  or the PLR. While  $M$  can be quickly configured as a  
 628 parameter setting within the device firmware or via a remote MAC command, the  
 629 PLR is not a directly configurable parameter since it depends on several variables,  
 630 as follows:

$$PLR = f(MAC, PHY, g, d), \quad (1.3)$$

631 As a matter of fact, it is worth noticing that the PLR depends on both  $MAC$  and  
 632  $PHY$  layer configurations. More specifically, a collision-free MAC strategy makes  
 633 the PLR only dependent on the Signal to Noise Ratio (SNR) [24]. Contrariwise,  
 634 when the MAC layer is contention-based, frames are correctly delivered if they  
 635 do not incur collisions. Moreover, the  $PHY$  layer configuration, such as LoRa's SF  
 636 value [12, 23] and NB-IoT's CE level, will also affect the PLR. With a higher SF value  
 637 or CE level, the maximum distance between EDs (UEs) and GW (eNB) increases.  
 638 Therefore, the  $PLR$  also increases with distance [39]. On the other hand, a broader  
 639 coverage area corresponds to a higher network load, which in turn increases the  
 640 collision probability [9]. In addition, the traffic generation rate  $g$  of each device and  
 641 the density of devices  $d$  also determine the network load. The collision can happen  
 642 in both the join and data transmission phase in the LoRaWAN [9, 38, 50] by using  
 643 the same SF at the same time in the specific channel. But for NB-IoT, the packet  
 644 loss caused by collision only occurs in the random-access phase. By increasing the  
 645 network load, allocating the limited network resources would be the main issue in  
 646 the NB-IoT. The resource allocation time (service time) may be too long in the  
 647 data transmission phase, also resulting in packet loss [11]. It has to be noticed that  
 648 the number of retransmissions can also be increased by the unavailability of the  
 649 network [4]. This is the case, for instance, of a satellite LoRa gateway: the device  
 650 may try to deliver several times the message to a network that it is not available.

Then, the time elapsed from the generation of the data frame to its correct

delivery (through a variable number of retransmissions) is the **Latency** of the network. It can be described as

$$L = f(MAC, t_p, \tilde{m}) \quad (1.4)$$

651 Without considering retransmissions, the different modes of the *MAC* protocol,  
 652 such as EDT mode for NB-IoT and Class B for LoRa, have different message  
 653 exchange strategies, thus giving various network latencies. Furthermore, differences  
 654 in the distance between the device and the GW (eNB) result in different propagation  
 655 times  $t_p$  [41], which are usually negligible for terrestrial networks (but considerable  
 656 for satellite networks). In fact, in the case of retransmissions caused by packet loss,  
 657 an extra delay will be added to the network, which depends on the average number of  
 658 retransmission  $\tilde{m}$ . *PLR* directly determines the expected number of retransmissions  
 659 required to transmit a packet successfully, and  $M$  provides an upper limit for this  
 660 number. So the average number of retransmission is

$$\tilde{m} = f(PLR, M). \quad (1.5)$$

661 Obviously, the parameters that affect the *PLR* also affect the latency, such as  
 662 the number of connected devices, CE level [7, 8], SF [9, 50], low SNR [40], etc.  
 663 As introduced in the previous part, when the *PLR* is high, a better way to keep  
 664 the network reliability is to increase the maximum number of retransmissions. But  
 665 as the maximum number of retransmissions increases, the network latency also  
 666 increases [37], so a trade-off strategy is needed based on the specific application  
 667 requirements.

The **Throughput** is the rate of successful packet delivery. The value of throughput is impacted by the traffic generated by each device, the network density, and *PLR*, as shown in equation 1.6. Obviously, the network with more density will have more generated traffic that also increases the *PLR*. Note that the ideal throughput is the generated traffic when *PLR* is equal to 0.

$$T = f(g, d, PLR) \quad (1.6)$$

668 For LoRa, several factors such as Inter-SF and Intra-SF [39] impact the throughput  
 669 by generating collisions due to orthogonality issues of the SFs. These factors will  
 670 reduce the throughput especially in networks with high node density, or co-existing  
 671 with other networks, or with large distance between the EDs and the GW [12]. In this  
 672 situation, an higher value of  $g$  will imply less throughput by increasing more ToA  
 673 and collision probability. Same for NB-IoT, the model of network throughput can be  
 674 built on the basis of *PLR* analysis [24]. The parameters such as the number of UEs  
 675 and traffic generation rate [40] are also critical factors that affect the throughput. On  
 676 the other hand, as the generated traffic increases, the system throughput will increase,



677 but the probability of collision will also increase, which has a negative impact on the  
 678 system throughput [49]. Therefore, an optimum scheduling technique can reach the  
 679 maximum available throughput by efficiently allocating the network resources [9].

The **Energy efficiency** describes the number of transmission bits obtained when the system consumes a unit of energy and presents the utilization efficiency of energy by the system [14]. Thus, the energy efficiency can be described as

$$EE = \frac{g_s}{E} = \frac{T}{N \times E}, \quad (1.7)$$

where  $g_s$  is the rate of successful transmissions for each device. In other words, its value is equal to the network throughput  $T$  divided by the total number of devices  $N$  in the network. Also the average energy consumption  $E$  depends on several parameters

$$E = f(PHY, MAC, \tilde{m}). \quad (1.8)$$

680 Like other KPIs, the number of retransmissions caused by high PLR directly  
 681 impacts the energy consumption rate, which requires extra energy to transmit fewer  
 682 packets per unit of time [40]. For NB-IoT, with the different CE levels based on  
 683 link quality, battery lifetime can be from 3 years to 23 years [7]. In the LoRaWAN,  
 684 the energy consumption is different based on the  $SF$  selection [41]. The lifetime  
 685 of an ED battery will be less than two years for the transmission interval of 60 s  
 686 with  $SF = 7$ , while it would be about 3 months for  $SF = 12$  [45]. The main goal  
 687 of the NB-IoT EDT mode is to simplify the transmission process, reducing energy  
 688 consumption. The model proposed in [10] focused on the energy consumption of the  
 689 UE, when working in EDT mode. The results show a significant improvement in the  
 690 performance. In the LoRaWAN, different classes have different energy consumption  
 691 behavior: Class A as the efficient, Class C as the thirsty, and Class B as the middle  
 692 energy consumer. Also, other variants were proposed in literature. For instance, Class  
 693 S was introduced in [17] to improved the performance of the Class B in throughput  
 694 and respectively energy efficiency by wisely enlarging the slots of Class B. Based on  
 695 Class S, TREMA [18] presented a scheduling technique to leverage from its energy  
 696 efficiency and higher throughput.

### ! Attention

697  
 698 Clearly, the best performance cannot be achieved for all the KPIs at the same  
 699 time. Therefore, a trade-off must be considered based on the needs of the specific  
 700 application. When considering a satellite LPWAN, the KPIs are affected by the  
 701 several challenges introduced by the LEO satellite. In what follows, the challenges  
 702 and their impact on the KPIs are discussed.

#### 704 **1.4 Satellite LPWAN: Opportunities and Challenges**

705 Satellite technology is emerging as a key enabler to transform IoT connectivity  
706 and allows global IoT coverage in beyond 5G systems [44, 47, 27]. By integrating  
707 satellites with long-range low power network technology, it is possible to deliver  
708 seamless connectivity, extended to air, sea [52], and other remote, difficult accessible  
709 areas. Besides extended coverage, the combination of satellites and LPWAN also  
710 gives the opportunity of increasing reliability and network capacity. In fact, satellites  
711 may be the only available communication medium when terrestrial networks are not  
712 available or not operational anymore (e.g., after a natural disaster).

713 Over the last years, IoT by satellite became more and more affordable, available,  
714 and accessible, thanks to the launch of several low-cost miniaturized Low Earth  
715 Orbit (LEO) satellites (CubeSats) [6]. Those LEO satellites are the most appealing  
716 ones for IoT applications due to the shorter delay that they introduce ( $\approx 40$  ms)  
717 compared to Geostationary Earth Orbit (GEO) satellites ( $\approx 500$  ms). However, their  
718 intrinsic orbital properties imply limited visibility time (around 2 minutes per visit).  
719 This issue can be overcome by using large constellations of LEO satellites, able to  
720 provide almost continuous coverage, and it will be further solved in future systems  
721 with relay networks from LEO to GEO satellites and inter-satellite links (ISL). The  
722 foreseen scenario is illustrated in Fig. 1.12.

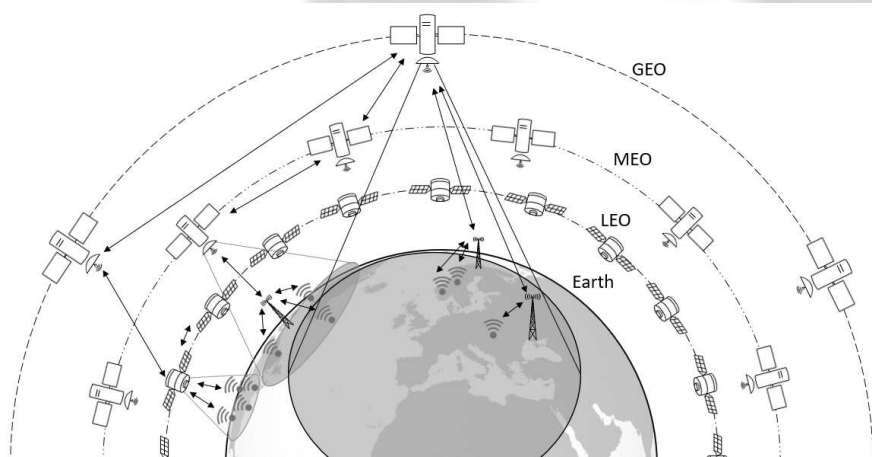


Fig. 1.12: Satellites on different orbits

723 Clearly, connecting IoT devices directly to LEO satellites opens many new op-  
724 portunities. Besides that, there exist many challenges to overcome for allowing the  
725 smooth integration and interoperability of satellites and LPWAN terrestrial net-  
726 works [30, 16]. This section overviews the challenges, while the following one will  
727 discuss their impact on the KPIs introduced in Sec. 1.3.

LEO satellites have large relative velocities to the IoT device on the ground, which results in a significant **Doppler effect**. For a LEO-600 km satellite, the maximum Doppler effect is up to  $\pm 48$  kHz [22], which is much larger than the bandwidth of one NB-IoT sub-carrier, equal to only 15 kHz. Moreover, the large distance between the IoT device on the ground and the LEO satellites (500 - 2000 km) introduces a higher **propagation delay**. In NB-IoT networks, UE and eNB must be synchronized in time and frequency. To this aim, several messages are exchanged between the UE and eNB (at least four in EDT mode) before the actual data transmission. Complete the synchronization and resource allocation phase within the limited visibility time of the satellite is a big challenge for NB-IoT. Due to the Doppler effect and long propagation delay, NB-IoT could easily fail to accomplish the message transmission. While LoRa does not request synchronization between the ED and the gateway prior to the data transmission, the Doppler effect still impacts the LoRa PHY protocol since CSS signals are extremely sensitive to time and frequency offsets. In [25], the authors demonstrated that SF 12 is more immune against the Doppler effect when EDs communicate with satellite gateways at a height above 500 Km. Recently, a modification of the LoRa PHY, namely the differential CSS (DCSS) was proposed in [13]. DCSS allows demodulating the signals without the need of performing a complete frequency synchronization and by tolerating some timing synchronization errors, such as those introduced by the Doppler shift, variable in time.

Long transmission distance, significantly attenuated electromagnetic waves, and high transmission loss are among the remarkable features of satellite communication. They all together determine the **link budget**, which impacts the energy consumption of the ground equipment, as well the KPIs of the entire system. For NB-IoT, lower spectral efficiency will affect the transmission of resource allocation information. It follows that the UE cannot transmit uplink data on time, which will result in decreased throughput and increased delay [36, 22]. Link budget from LoRa ground sensor to satellite gateway has been computed empirically in literature [28], confirming the feasibility of the communication. Both LoRa PHY with SF 12 and LR-FHSS protocol allow increasing network capacity and collision robustness against link budget constraints [15].

As distance increases, ground devices must consume more power than what is needed in terrestrial systems to send or receive messages. This translates into a shorter battery lifetime for the NB-IoT UEs [36]. The same applies to LoRa EDs. In [29], the authors evaluated the performance of a satellite LoRaWAN using Iridium Satellites: they proved that EDs with a battery of 2400 mAh could operate  $\sim 1$  year, transmitting every 100 minutes. To increase the battery lifetime, the transmission rate should be decreased, which translates in reduced throughput.

A large constellation of LEO satellites with inter-satellite-links (as illustrated in Fig. 1.12) can provide full and continuous coverage to IoT devices on the earth. Such seamless connectivity comes with increased cost and complexity of the network. A more feasible solution consists of **discontinuous communication** with a small constellation of few LEO satellites [51]. In such a scenario with intermittent connectivity, to save energy the IoT devices must wake up and transmit only when the satellite is available. Following the NB-IoT specifications, the synchronization signal must

773 be received before the data transmission. In Rel. 17, 3GPP proposed the use of the  
 774 Global Navigation Satellite System (GNSS) signal for the UE to compute the satel-  
 775 lites and their own position. This method can pre-compensate for the Doppler effect,  
 776 the frequency and time offset caused by the long distance. Those advantages come at  
 777 the price of high energy consumption. Another solution proposed in literature [21]  
 778 makes use of the synchronization signal transmitted in each NB-IoT downlink radio  
 779 frame to inform on time the ground UEs about the arrival time of the satellite. Even  
 780 though LoRa, unlike NB-IoT, does not request any synchronization prior to the data  
 781 transmission, the EDs must be aware of the satellite passes to avoid wasting energy  
 782 in unsuccessful transmissions. To this aim, the EDs must have access to the Two-  
 783 Line Element (TLE) data of the satellite (see Fig. 1.13). The TLE provides a set of  
 784 algebraic information, i.e., the satellite orbital elements, which allow predicting the  
 785 satellite trajectory over time. Due to deviations from its initial orbit, the TLE data  
 786 must be updated periodically. Current satellite LoRaWAN solutions available on the  
 787 market make use of the TLE data <sup>10</sup>. Due to the considerable number of EDs that  
 788 could be in the satellite coverage (i.e., within the satellite footprint), the knowledge  
 789 of the satellite passes is not enough to ensure good network performance. In fact, the  
 790 probability of collision, already high in LoRaWAN terrestrial networks [9], could  
 791 only get worst in such a hybrid scenario. It follows the need of adopting scheduling  
 792 techniques [5] to avoid collisions. In addition, *bulk data transmission* [53] could be  
 793 used in combination with TDMA approaches to ensure efficient use of the limited  
 794 satellite resources (2-3 times visibility per day, for approximately 2 minutes.).

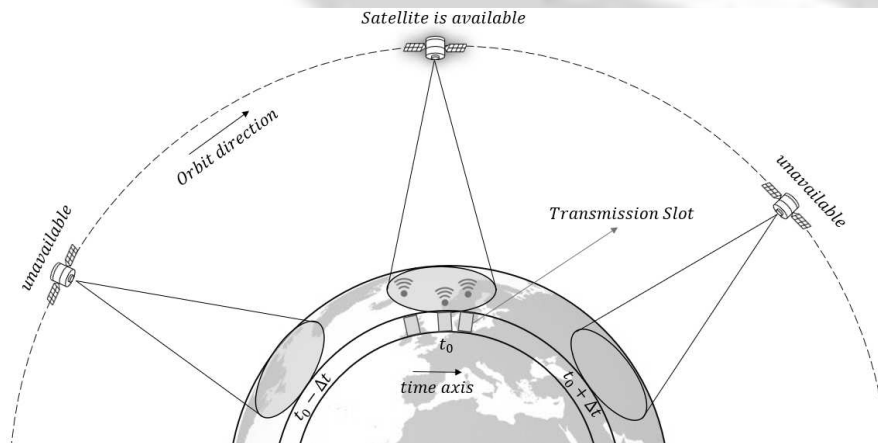


Fig. 1.13: LEO satellite coverage, while moving along its orbit. The knowledge of the satellite TLE allows the EDs to transmit when they are in the coverage range of the satellite (i.e., within the satellite footprint).

<sup>10</sup> Lacuna Space: <https://lacuna.space/>

795 The unavailability of the satellite does not affect only the access network. The  
 796 communication between the satellite and the network server can be discontinuous  
 797 too. To ensure end-to-end communication over the entire network, and avoid packet  
 798 drops, the satellite gateway or satellite eNB must have the ability to store the messages  
 799 and forward them when passing through the ground satellite gateway. The lack of  
 800 connectivity between the satellite and the LNS can also hamper the exchange of  
 801 LoRa confirmed uplink messages. Even in the case of correct reception of the packet  
 802 at the LNS, in absence of ACK (not forwarded at all by the gateway because not  
 803 available, either not transmitted on time, within the receiving windows), the ED  
 804 would retry the transmission. This results in the wasting of resources: ED's energy,  
 805 channel resources with contention, and possible collision with other concurrent  
 806 transmissions. Overall, it translates to deterioration of the network performance in  
 807 terms of reliability, throughput, and energy efficiency.

### 808 Tips

809 Discontinuous communication can also cause network authentication problems.  
 810 In a NB-IoT network, the network authentication is unfeasible when the UE and  
 811 the ground base station are not in the same satellite coverage at the same time.  
 812 Discontinuous communication makes the handshake between the UE and the core  
 813 network impossible, which poses a challenge to the reliability of the satellite IoT.  
 814 Like NB-IoT, the LoRaWAN OTAA join procedure would fail when EDs and LNS  
 815 are not at the same time under the coverage of the satellite gateway [4]. Moreover,  
 816 stable connectivity is needed to support downlink multicast traffic. Prior to the  
 817 multicast data exchange, several uplink and downlink unicast messages must be  
 818 exchanged between the EDs and the LNS (multicast session set-up). Intermittent  
 819 links would cause the expiration of multicast session timeouts and would thus prevent  
 820 the multicast transmission.

## 822 1.5 Qualitative Performance Analysis of Satellite LPWAN

823 In Section 1.3, some KPIs for the performance evaluation of terrestrial LPWAN  
 824 networks were analyzed. However, when integrating LPWAN with LEO satellites, the  
 825 challenges presented in Section 1.4 must be taken into account to model and estimate  
 826 the KPIs of the combined network. In this section, the analysis presented is referred  
 827 to the availability of a single satellite equipped either with a LoRa GW or a NB-IoT  
 828 eNB. This represents the worst case scenario. Instead, LEO constellations will be  
 829 considered in future works to feature the scalability of such network architecture.

830 First, it has to be noticed that the **reliability** of the satellite LPWAN network would  
 831 be highly affected by the LEO satellite and its visibility time. In fact, a major source  
 832 of packet losses is caused by the frequent unavailability of the LoRa GW (eNB). Let  
 833  $a_S$  be the satellite availability. Then, the reliability of the satellite LPWAN  $R_S$  is

$$R_s = R \times a_S. \quad (1.9)$$

834 Clearly,  $R_s$  as  $R$  is mainly a function of the PLR. The latter can still be formulated  
 835 as in equation 1.3. Thus, it is dependent by PHY and MAC parameters, traffic  
 836 generation rate per node, and node density. Thanks to its large footprint, the LEO  
 837 satellite can provide wide coverage, resulting in a large number of IoT devices being in  
 838 the satellite visibility at the same time. The higher value of the node density increases  
 839 the  $PLR$ , and thus deteriorates the reliability. When considering a constellation of  
 840 LEO satellites, offering continuous coverage, it results  $a_S \rightarrow 1$ , and thus,  $R_s \rightarrow R$ .

841 The **Latency** of the network, as expressed in Equation 1.4, is affected by the  
 842 MAC schemes, together with the propagation time, and the average number of  
 843 retransmissions. More in details, the Latency is the combination of different delays,  
 844 due to the initial synchronization, the following data processing and propagation,  
 845 and finally the data delivery to the application sever over the satellite backhaul. In a  
 846 simplified manner, the Latency  $L_s$  can be formulated as:

$$L_s = t_{sync} + m \times (t_{pr} + t_p) + t_{sb} \quad (1.10)$$

847 with  $m$  representing the total number of packet exchanged, including retransmis-  
 848 sions. A device takes  $t_{pr}$  to generate a packet, which will propagate for  $t_p$  to be  
 849 received by the gateway. Ground-to-satellite links are featured by a larger propaga-  
 850 tion delay  $t_p$  than that of terrestrial networks. Besides, such a delay is not fixed and  
 851 its duration varies according to satellite movements. Meanwhile, the packet takes  
 852  $t_{sb}$  to be delivered from the satellite gateway till the remote sever. In case of a LEO  
 853 satellite constellation,  $t_{sb}$  includes the ISL link delay. The network latency increases  
 854 according to growing numbers of ISL.

855 For LoRa unconfirmed messages, the Equation 1.10 is simplified, with  $m = 1$   
 856 and  $t_{sync} = 0$ . For NB-IoT, the synchronization delay is a relevant component of  
 857 the satellite network latency. Moreover,  $m$  varies according to the different NB-IoT  
 858 optimization modes (UP, CP, EDT). In case of higher PLR, the value of  $m$  will  
 859 increase, resulting in higher latency. Being the confirmed messages acknowledged  
 860 directly by the eNB, no additional delay is introduced by the satellite backhaul.

861 As the reliability, also the **Throughput** is affected by the satellite availability time  
 862 and large coverage range. So it can be described by equation 1.11. Unavailability  
 863 of the satellite causes more packet losses and therefore less throughput. Similarly,  
 864 having many devices (with higher density  $d$ ) in the coverage range of the satellite  
 865 translates in higher PLR, due to data packet collision in LoRa, and congestion during  
 866 NB-IoT synchronization. As consequence of increased PLR, the throughput of the  
 867 satellite LPWAN decreases.

$$T_s = T \times a_S \quad (1.11)$$

868 The communication with a satellite gateway strongly impacts the energy con-  
 869 sumption of the IoT device on the ground. The long distance between the device and  
 870 the satellite asks for more power consumption, both in transmission and  $E_{TX}$ , and

871 reception mode  $E_{RX}$ . Instead, the energy required for processing the message,  $E_{pr}$   
 872 remains the same as in fully terrestrial networks. Thus, the energy consumption can  
 873 be described as

$$E_{total} = E_{sync} + m_1 \times (E_{pr} + E_{TX}) + m_2 \times (E_{pr} + E_{RX}), \quad (1.12)$$

874 where  $m_1$  and  $m_2$  represent the number of uplink and downlink packets, respectively.

875 For unconfirmed LoRa message, the equation 1.12 is simplified, by considering  
 876  $m_1 = 1$ ,  $m_2 = 0$  and  $E_{sync} = 0$ . In case of LoRa confirmed messages, then  $m_1 = m_2$   
 877 and  $m_1$  represent the number of retransmissions,  $m - 1$ . In a NB-IoT network, the  
 878 value of  $m_1$  and  $m_2$  change based on the different optimization method adopted.  
 879 Moreover, the energy spent during the synchronization phase  $E_{sync}$  represents a  
 880 relevant component of the whole energy consumption of the IoT device.

881 As mentioned in the previous section, one LEO satellite suffers from long unavail-  
 882 ability times during a specific time period. Such behaviour makes satellite LPWAN  
 883 not fit the applications that require higher reliability (like mission-critical, Tactile  
 884 Internet, etc.) . Since the satellite has a broader coverage area, more devices will  
 885 try to connect to the satellite at the same time, and the probability of collision will  
 886 be greatly increased. As a result, applications requiring high throughput cannot be  
 887 satisfied. Therefore, the network size (i.e., the number of served devices) should be  
 888 reduced, to increase the network throughput. Finally, satellites impose the network  
 889 to have longer delays and thus longer latency comparing to the terrestrial networks.  
 890 This makes them not a good fit for ultra low latency applications. While the goal  
 891 of any network is to support higher scalability, then increasing the number of LEO  
 892 satellites and providing a full coverage will help supporting the applications that  
 893 need higher reliability and throughput.

## 894 1.6 Conclusion and Future work

895 NB-IoT and LoRaWAN are among the LPWAN technologies that have fostered  
 896 a widespread deployment of IoT networks, thanks to their low power, low cost  
 897 and long distance communications. These features have recently been explored for  
 898 ground-to-satellite communications, enabling a truly pervasive and ubiquitous IoT  
 899 availability. Such a network architecture is clearly expected to trigger the growth of  
 900 novel IoT applications unimaginable before. Indeed, the success of the future satellite  
 901 IoT will come from its ability to meet the needs of specific use cases. Timely, this  
 902 chapter pictures a methodological approach finalized to the correct choice of the  
 903 LPWAN technology and the best communication pattern fitting the needs of *any*  
 904 satellite IoT application. To do that, reliability, latency, throughput, and energy  
 905 efficiency have been identified as KPIs to be used for comparing different protocols.  
 906 Importantly, their inner dependency on configurable setting, e.g., the maximum  
 907 number of retransmissions in contention-based medium access schemes, has also  
 908 been properly investigated. Such an analysis will be leveraged in future research

909 works to design both novel medium access schemes, and efficient algorithms able to  
 910 autonomously adapt the communication protocol to time-varying traffic conditions  
 911 and to grant a sufficient level of quality of service. In addition, such an analysis will  
 912 be extended to tackle the availability of LEO satellite constellations, thus targeting  
 913 highly available and scalable LPWANs backhauled by LEO satellites.

914 **Acknowledgements** This work was supported by the IRT Saint Exupéry project satELLite IOT  
 915 (ELLIOT), the ANR LabEx CIMI (grant ANR-11-LABX-0040) within the French State Pro-  
 916 gramme “Investissements d’Avenir,” the Project STICAMSUD 21-STIC-12, and the Design of  
 917 LoRaWAN protocol optimisation over SATellite Connection for precision agriculture applica-  
 918 tions (LORSAT) Project, through the National Research Fund Luxembourg (FNR), under Grant  
 919 CORE/C19/IS/13705191.

Table 1.3: Symbol definitions

Symbol	Definition
$g$	Traffic generation rate per single node
$g_r$	Traffic successful transmission rate per single node
$PHY$	PHY layer configurations
$MAC$	MAC layer configurations
$t_p$	Propagation time between the device and the gateway
$t_{pr}$	Message Processing time
$t_{sb}$	Delivery Time over the Satellite backhaul, from the satellite to the server
$t_{sync}$	Synchronization Time between the UE and eNB
$E$	Device energy consumption
$EE$	Energy Efficiency of the network
$E_{sync}$	Energy spent for the synchronization
$E_{TX}$	Energy consumption in TX mode
$E_{RX}$	Energy consumption in RX mode
$E_{pr}$	Energy consumption for processing the data
$E_{total}$	Total energy required to deliver the message to the satellite
$a_s$	Satellite availability rate during a specific period
$DR$	Message Data Rate
$d$	Density of devices operating in the network
$N$	Number of devices operating in the network
$M$	Maximum number of retransmissions
$\bar{m}$	Average number of retransmission
$r_t$	Number of retransmissions
$L$	e2e LPWAN network latency
$L_s$	e2e satellite LPWAN network latency
$T$	e2e LPWAN network throughput
$T_s$	e2e satellite LPWAN network throughput
$R$	e2e LPWAN network reliability
$R_s$	e2e satellite LPWAN network reliability



## 920 References

- 921 1. Sigfox, Available online:<https://www.sigfox.com/en>. Accessed on 1 May 2022
- 922 2. Standards for the IoT, Available online:[https://www.3gpp.org/news-events/1805-iot\\_r14](https://www.3gpp.org/news-events/1805-iot_r14). Ac-  
923 cessed on 2 dec 2016
- 924 3. What Is LoRa®?, available online: <https://www.semtech.com/lora/what-is-lora>. Accessed on  
925 1 Feb 2022
- 926 4. Afhamisis, M., Barillaro, S., Palattella, M.: A Testbed for Lorawan Satellite Backhaul: Design  
927 Principles and Validation. In: ICC 2021 - IEEE International Conference on Communications.  
928 IEEE (2022)
- 929 5. Afhamisis, M., Palattella, M.R.: SALSA: A Scheduling Algorithm for LoRa to LEO Satellites.  
930 IEEE Access **10**, 11608–11615 (2022). DOI 10.1109/ACCESS.2022.3146021
- 931 6. Akyildiz, I.F., Kak, A.: The Internet of Space Things, CubeSats: A ubiquitous cyber physical  
932 system for the connected world. Computer Networks **150**, 134–149 (2019). DOI 10.1016/j.  
933 comnet.2018.12.017
- 934 7. Andres-Maldonado, P., Lauridsen, M., Ameigeiras, P., Lopez-Soler, J.M.: Analytical Modeling  
935 and Experimental Validation of NB-IoT Device Energy Consumption. IEEE Internet of Things  
936 Journal **6**(3), 5691–5701 (2019). DOI 10.1109/JIOT.2019.2904802
- 937 8. Azari, A., Stefanović, v., Popovski, P., Cavdar, C.: On the Latency-Energy Performance of  
938 NB-IoT Systems in Providing Wide-Area IoT Connectivity. IEEE Transactions on Green  
939 Communications and Networking **4**(1), 57–68 (2020). DOI 10.1109/TGCN.2019.2948591
- 940 9. Bankov, D., Khorov, E., Lyakhov, A.: LoRaWAN Modeling and MCS Allocation to Satisfy  
941 Heterogeneous QoS Requirements. Sensors **19**(19) (2019). DOI 10.3390/s19194204
- 942 10. Barbau, R., Deslandes, V., Jakllari, G., Beylot, A.: An Analytical Model for Evaluating  
943 the Interplay Between Capacity and Energy Efficiency in NB-IoT. In: 2021 International  
944 Conference on Computer Communications and Networks (ICCCN), pp. 1–9 (2021). DOI  
945 10.1109/ICCCN52240.2021.9522178
- 946 11. Barbau, R., Deslandes, V., Jakllari, G., Tronc, J., Beylot, A.: An Analytical Model for Assessing  
947 the Performance of NB-IoT. In: ICC 2021 - IEEE International Conference on Communica-  
948 tions, pp. 1–6 (2021). DOI 10.1109/ICC42927.2021.9500950
- 949 12. Beltramelli, L., Mahmood, A., Gidlund, M., Österberg, P., Jennehag, U.: Interference Mod-  
950 elling in a Multi-Cell LoRa System. In: 2018 14th International Conference on Wireless  
951 and Mobile Computing, Networking and Communications (WiMob), pp. 1–8 (2018). DOI  
952 10.1109/WiMOB.2018.8589100
- 953 13. Ben Temim, M.A., Ferré, G., Tajan, R.: A New LoRa-like Transceiver Suited for LEO Satellite  
954 Communications. Sensors **22**(5) (2022). DOI 10.3390/s22051830
- 955 14. Björnson, E., Larsson, E.G.: How Energy-Efficient Can a Wireless Communication System  
956 Become? In: 2018 52nd Asilomar Conference on Signals, Systems, and Computers, pp.  
957 1252–1256 (2018). DOI 10.1109/ACSSC.2018.8645227
- 958 15. Boquet, G., Tuset-Peiró, P., Adelantado, F., Watteyne, T., Vilajosana, X.: LR-FHSS: Overview  
959 and Performance Analysis. IEEE Communications Magazine **59**(3), 30–36 (2021). DOI  
960 10.1109/MCOM.001.2000627
- 961 16. Centenaro, M., Costa, C., Granelli, F., Sacchi, C., Vangelista, L.: A Survey on Technologies,  
962 Standards and Open Challenges in Satellite IoT. IEEE Communications Surveys Tutorials  
963 **23**(3), 1693–1720 (2021). DOI 10.1109/COMST.2021.3078433
- 964 17. Chasserat, L., Accettura, N., Berthou, P.: Short: Achieving Energy Efficiency in Dense Lo-  
965 RaWANs through TDMA. In: 2020 IEEE 21st International Symposium on "A World  
966 of Wireless, Mobile and Multimedia Networks" (WoWMoM), pp. 26–29 (2020). DOI  
967 10.1109/WoWMoM49955.2020.00019
- 968 18. Chasserat, L., Accettura, N., Prabhu, B., Berthou, P.: TREMA: A traffic-aware energy  
969 efficient MAC protocol to adapt the LoRaWAN capacity. In: 2021 International Con-  
970 ference on Computer Communications and Networks (ICCCN), pp. 1–6 (2021). DOI  
971 10.1109/ICCCN52240.2021.9522147

- 972 19. Chaudhari, B.S., Zennaro, M., Borkar, S.: LPWAN Technologies: Emerging Application Char-  
973 characteristics, Requirements, and Design Considerations. *Future Internet* **12**(3) (2020). DOI  
974 10.3390/fi12030046
- 975 20. Chen, Y., Sambo, Y.A., Onireti, O., Imran, M.A.: A Survey on LPWAN-5G Integration:  
976 Main Challenges and Potential Solutions. *IEEE Access* **10**, 32132–32149 (2022). DOI  
977 10.1109/ACCESS.2022.3160193
- 978 21. Chougrani, H., Kisseleff, S., Martins, W.A., Chatzinotas, S.: NB-IoT Random Access for  
979 Non-Terrestrial Networks: Preamble Detection and Uplink Synchronization. *IEEE Internet of  
980 Things Journal* pp. 1–1 (2021). DOI 10.1109/JIOT.2021.3123376
- 981 22. Conti, M., Andrenacci, S., Maturo, N., Chatzinotas, S., Vanelli-Coralli, A.: Doppler Impact  
982 Analysis for NB-IoT and Satellite Systems Integration. In: *ICC 2020 - 2020 IEEE Interna-  
983 tional Conference on Communications (ICC)*, pp. 1–7 (2020). DOI 10.1109/ICC40277.2020.  
984 9149140
- 985 23. Croce, D., Gucciardo, M., Mangione, S., Santaromita, G., Tinnirello, I.: Impact of LoRa  
986 Imperfect Orthogonality: Analysis of Link-Level Performance. *IEEE Communications Letters*  
987 **22**(4), 796–799 (2018). DOI 10.1109/LCOMM.2018.2797057
- 988 24. Cruz, R., Coelho, A., Campos, R., Ricardo, M.: A Theoretical Model for Planning NB-IoT  
989 Networks. In: *2019 International Conference on Wireless and Mobile Computing, Networking  
990 and Communications (WiMob)*, pp. 1–4 (2019). DOI 10.1109/WIMOB.2019.8923389
- 991 25. Doroshkin, A.A., Zadorozhny, A.M., Kus, O.N., Prokopyev, V.Y., Prokopyev, Y.M.: Experimen-  
992 tal Study of LoRa Modulation Immunity to Doppler Effect in CubeSat Radio Communications.  
993 *IEEE Access* **7**, 75721–75731 (2019). DOI 10.1109/ACCESS.2019.2919274
- 994 26. ETSI (European Telecommunications Standards Institute): System Reference document (SR-  
995 doc); Technical characteristics for Low Power Wide Area Networks Chirp Spread Spectrum  
996 (LPWAN-CSS) operating in the UHF spectrum below 1 GHz. Tech. Rep. TR 103 526 V1.1.1,  
997 Washington, DC, USA (2018 [Online]). URL {<https://www.etsi.org/>}
- 998 27. Fang, X., Feng, W., Wei, T., Chen, Y., Ge, N., Wang, C.X.: 5G Embraces Satellites for 6G  
999 Ubiquitous IoT: Basic Models for Integrated Satellite Terrestrial Networks. *IEEE Internet of  
1000 Things Journal* **8**(18), 14399–14417 (2021). DOI 10.1109/JIOT.2021.3068596
- 1001 28. Fernandez, L., Ruiz-De-Azua, J.A., Calveras, A., Camps, A.: Assessing LoRa for Satellite-to-  
1002 Earth Communications Considering the Impact of Ionospheric Scintillation. *IEEE Access* **8**,  
1003 165570–165582 (2020). DOI 10.1109/ACCESS.2020.3022433
- 1004 29. Gomez, C., Darroudi, S.M., Naranjo, H., Paradells, J.: On the Energy Performance of Iridium  
1005 Satellite IoT Technology. *Sensors* **21**(21) (2021). DOI 10.3390/s21217235
- 1006 30. Guidotti, A., Vanelli-Coralli, A., Conti, M., Andrenacci, S., Chatzinotas, S., Maturo, N., Evans,  
1007 B., Awoseyila, A., Ugolini, A., Foggi, T., Gaudio, L., Alagha, N., Cioni, S.: Architectures  
1008 and key technical challenges for 5g systems incorporating satellites. *IEEE Transactions on  
1009 Vehicular Technology* **68**(3), 2624–2639 (2019). DOI 10.1109/TVT.2019.2895263
- 1010 31. Guo, Y., Zhang, D.: Research on the Reliability of MAC Protocols for Multi-radio Sensor  
1011 Networks. In: *2010 First International Conference on Pervasive Computing, Signal Processing  
1012 and Applications*, pp. 410–413 (2010). DOI 10.1109/PCSPA.2010.105
- 1013 32. Harwahu, R., Cheng, R.G., Liu, D.H., Sari, R.F.: Fair Configuration Scheme for Random  
1014 Access in NB-IoT with Multiple Coverage Enhancement Levels. *IEEE Transactions on Mobile  
1015 Computing* **20**(4), 1408–1419 (2021). DOI 10.1109/TMC.2019.2962422
- 1016 33. Høglund, A., Van, D.P., Tirronen, T., Liberg, O., Sui, Y., Yavuz, E.A.: 3GPP Release 15  
1017 Early Data Transmission. *IEEE Communications Standards Magazine* **2**(2), 90–96 (2018).  
1018 DOI 10.1109/MCOMSTD.2018.1800002
- 1019 34. Jiao, J., Wu, S., Lu, R., Zhang, Q.: Massive Access in Space-Based Internet of Things:  
1020 Challenges, Opportunities, and Future Directions. *IEEE Wireless Communications* **28**(5),  
1021 118–125 (2021). DOI 10.1109/MWC.001.2000456
- 1022 35. Knight, M., Seeber, B.: Decoding LoRa: Realizing a Modern LPWAN with SDR. *Proceedings  
1023 of the GNU Radio Conference* **1**(1) (2016)
- 1024 36. Kodheli, O., Maturo, N., Andrenacci, S., Chatzinotas, S., Zimmer, F.: Link Budget Analysis  
1025 for Satellite-Based Narrowband IoT Systems. In: *Ad-Hoc, Mobile, and Wireless Networks*,  
1026 pp. 259–271. Springer International Publishing (2019)

- 1027 37. Li, H., Chen, G., Wang, Y., Gao, Y., Dong, W.: Accurate Performance Modeling of Uplink  
1028 Transmission in NB-IoT. In: 2018 IEEE 24th International Conference on Parallel and Dis-  
1029 tributed Systems (ICPADS), pp. 910–917 (2018). DOI 10.1109/PADSW.2018.8644571
- 1030 38. Mahmood, A., Sisinni, E., Guntupalli, L., Rondón, R., Hassan, S.A., Gidlund, M.: Scalability  
1031 Analysis of a LoRa Network Under Imperfect Orthogonality. *IEEE Transactions on Industrial*  
1032 *Informatics* **15**(3), 1425–1436 (2019). DOI 10.1109/TII.2018.2864681
- 1033 39. Markkula, J., Mikhaylov, K., Haapola, J.: Simulating LoRaWAN: On Importance of Inter  
1034 Spreading Factor Interference and Collision Effect. In: IEEE International Conference on  
1035 Communications (ICC), pp. 1–7 (2019). DOI 10.1109/ICC.2019.8761055
- 1036 40. Migabo, E., Djouani, K., Kurien, A.: A Modelling Approach for the Narrowband IoT (NB-  
1037 IoT) Physical (PHY) Layer Performance. In: IECON - 44th Annual Conference of the IEEE  
1038 Industrial Electronics Society, pp. 5207–5214 (2018). DOI 10.1109/IECON.2018.8591281
- 1039 41. Nurgaliyev, M., Saymbetov, A., Yashchyshyn, Y., Kuttybay, N., Tukymbekov, D.: Prediction  
1040 of energy consumption for LoRa based wireless sensors network. *Wireless Networks* **26**(5),  
1041 3507–3520 (2020). DOI 10.1007/s11276-020-02276-5
- 1042 42. Oliveira, R., Guardalben, L., Sargento, S.: Long Range Communications in Urban and Rural  
1043 environments. In: IEEE Symposium on Computers and Communications (ISCC), pp. 810–817  
1044 (2017). DOI 10.1109/ISCC.2017.8024627
- 1045 43. Palattella, M.R., Accettura, N.: Enabling Internet of Everything Everywhere: LPWAN with  
1046 Satellite Backhaul. In: Global Information Infrastructure and Networking Symposium (GIIS),  
1047 pp. 1–5 (2018). DOI 10.1109/GIIS.2018.8635663
- 1048 44. Palattella, M.R., O’Sullivan, J., Pradas, D., McDonnell, K., Rodriguez, I., Karagiannis, G.: 5G  
1049 Smart Connectivity Platform for Ubiquitous and Automated Innovative Services. In: IEEE  
1050 32nd Annual International Symposium on Personal, Indoor and Mobile Radio Communications  
1051 (PIMRC), pp. 1582–1588 (2021). DOI 10.1109/PIMRC50174.2021.9569463
- 1052 45. Philip, M.S., Singh, P.: Energy Consumption Evaluation of LoRa Sensor Nodes in Wireless  
1053 Sensor Network. In: Advanced Communication Technologies and Signal Processing (ACTS),  
1054 pp. 1–4 (2021). DOI 10.1109/ACTS53447.2021.9708341
- 1055 46. Polonelli, T., Brunelli, D., Marzocchi, A., Benini, L.: Slotted ALOHA on LoRaWAN-Design,  
1056 Analysis, and Deployment. *Sensors* **19**(4), 838 (2019). DOI 10.3390/s19040838
- 1057 47. Qu, Z., Zhang, G., Cao, H., Xie, J.: LEO Satellite Constellation for Internet of Things. *IEEE*  
1058 *Access* **5**, 18391–18401 (2017). DOI 10.1109/ACCESS.2017.2735988
- 1059 48. Soret, B., Mogensen, P., Pedersen, K.I., Aguayo-Torres, M.C.: Fundamental tradeoffs among  
1060 reliability, latency and throughput in cellular networks. In: IEEE Globecom Workshops (GC  
1061 Wkshps), pp. 1391–1396 (2014). DOI 10.1109/GLOCOMW.2014.7063628
- 1062 49. Sun, Y., Tong, F., Zhang, Z., He, S.: Throughput Modeling and Analysis of Random Access  
1063 in Narrowband Internet of Things. *IEEE Internet of Things Journal* **5**(3), 1485–1493 (2018).  
1064 DOI 10.1109/JIOT.2017.2782318
- 1065 50. Sørensen, R.B., Kim, D.M., Nielsen, J.J., Popovski, P.: Analysis of Latency and MAC-Layer  
1066 Performance for Class A LoRaWAN. *IEEE Wireless Communications Letters* **6**(5), 566–569  
1067 (2017). DOI 10.1109/LWC.2017.2716932
- 1068 51. Tondo, F.A., Montejo-Sánchez, S., Pellenz, M.E., Céspedes, S., Souza, R.D.: Direct-to-Satellite  
1069 IoT Slotted Aloha Systems with Multiple Satellites and Unequal Erasure Probabilities. *Sensors*  
1070 **21**(21) (2021). DOI 10.3390/s21217099
- 1071 52. Wei, T., Feng, W., Chen, Y., Wang, C.X., Ge, N., Lu, J.: Hybrid Satellite-Terrestrial Com-  
1072 munication Networks for the Maritime Internet of Things: Key Technologies, Opportuni-  
1073 ties, and Challenges. *IEEE Internet of Things Journal* **8**(11), 8910–8934 (2021). DOI  
1074 10.1109/JIOT.2021.3056091
- 1075 53. Zorbas, D., Caillouet, C., Abdelfadeel Hassan, K., Pesch, D.: Optimal Data Collection Time in  
1076 LoRa Networks—A Time-Slotted Approach. *Sensors* **21**(4) (2021). DOI 10.3390/s21041193